INFRASOUND SIGNAL CHARACTERISTICS FROM SMALL EARTHQUAKES

J. Mark Hale[1], Stephen J. Arrowsmith[2], Chris Hayward[3], Relu Burlacu[1], Kristine L. Pankow[1], Brian W. Stump[3], George E. Randall[2], and Steven R. Taylor[4]

University of Utah[1], Los Alamos National Laboratory[2], Southern Methodist University[3], and Rocky Mountain Geophysics[4]

Sponsored by the National Nuclear Security Administration

Award No. DE-AR52-08NA28608
Proposal No. BAA09-49

ABSTRACT

Understanding the source properties responsible for infrasound generation is critical to developing a seismo-acoustic data discriminant to distinguish between near-surface explosions and earthquakes. The regional seismicity, complex topography, open-pit quarries, and subsurface mining in the Utah region create a unique setting for the study of near-field infrasound. The Utah network has been operating three permanent infrasound arrays collocated with seismic stations NOQ (2006), BGU (2007), and EPU (2007). Additionally, four new arrays were installed and collocated with existing seismic stations BRPU, FSUT, HWUT, and WMUT. This summer three additional arrays will be collocated at stations LCMT, PSUT, and RCJ. Each array consists of four infrasound sensors with an average spacing of ~100 m, recording at 100 samples/s, and all data is telemetered to the University of Utah in near-real-time. This increased array coverage provides greater likelihood for independent locations of infrasound sources using crossing backazimuth estimates. The data from the arrays are being processed with InfraMonitor, which generates lists of detections and catalogs of located infrasound sources. Once processing is complete, the detections will be used to correlate and model the infrasound generation by earthquakes utilizing preexisting earthquake scaling relations dependent on depth, magnitude, and mechanism. The observations made during this study will contribute to refining the source excitation model for infrasound.

OBJECTIVES

An understanding of the mechanism involved in infrasound generation by earthquakes is critical for the development of seismo-acoustic discriminants that distinguish between surface explosions and earthquakes. The generation of infrasound from surface explosions has been documented by many groups, e.g., McKenna et al. (2007), Che et al. (2002), and Sorrells et al. (1997). These studies show that infrasound detections can be path dependent (Arrowsmith et al., 2008) and depend on time-varying atmospheric conditions (Garcés et al., 1998). These results suggest that with just a single array many potential infrasound detections might go unrecorded. Previous studies on earthquake-generated infrasound have largely been limited to medium-to-large earthquakes recorded at distances greater than 220 km (e.g., Kim et al., 2004, Mutschlecner and Whitaker, 2005, and Le Pichon et al., 2006). From these studies there is a suggestion of a linear relationship between earthquake magnitude (M > 4) and the duration of stratospheric returns as well as a linear relationship between earthquake magnitude and the log of amplitude for stratospheric returns corrected for winds and scaled to a reference distance (Mutschlecner and Whitaker, 2005 and Le Pichon et al., 2006).

Due to the sparseness of historical infrasound deployments, most previous studies of earthquake-generated infrasound studies have focused on only single-array observations; consideration of magnitude scaling relations, while neglecting the effects of earthquake depth, focal mechanism, and local geology; large earthquakes, omitting earthquakes M < 4; and observations limited to distances > 220 km. The goal of this project is to expand on previous work as follows:

- **Installing a dense network of seismo-acoustic arrays within 220 km of a major earthquake zone.** All of the arrays are (or will be installed) in the state of Utah within ~115 km of the axis of the Intermountain Seismic Belt (Smith and Arabasz, 1991), a zone of seismicity that extends from Nevada and Arizona northeast to Montana (Figure 1). In addition to the seismicity, the region is marked by complex topography, open-pit quarries, and subsurface coal mining, resulting in diverse seismo-acoustic signals. The network design should reduce the sensitivity to path effects documented from the previous explosion studies and increase the likelihood of acquiring detections on multiple arrays, which will allow robust associations with seismic events (Arrowsmith et al., 2008). The close distance to the sources will allow for analysis of infrasound propagation in the shadow zone where standard atmospheric models predict no infrasound arrivals and where Stump et al. (2007) observed strong variability in infrasound amplitudes.
- **Extending the analysis to earthquakes with M < 4.0.** This will be done to determine if similar linear scaling documented by Mutschlecner and Whitaker (2005) and Le Pichon et al. (2006) holds for the smaller magnitudes and if there exists a threshold magnitude or minimum ground motion for generating infrasound.
- **Analyzing source characteristics and earthquake ground motions for earthquakes generating infrasound**. Earthquakes will be analyzed to determine peak ground motions using a combination of observations and predictive ground-motion relations, to refine depth estimates, and, when possible, to determine source mechanisms with a goal of relating these additional source characteristics to the infrasound observations.

Here we report on progress to date that includes the installation of the new arrays, details of the routine data processing that will be applied to the new dataset, and preliminary analysis from two days of processing, each day containing a significant event.

RESEARCH ACCOMPLISHED

Deployment

Network design and array installation have been the focus during this first year of a three-year project. The original plan was to add three arrays to the existing network (NOQ, BGU, and EPU) of infrasound arrays embedded in the Utah Regional Seismic Network (Stump et al., 2009), which were installed in 2006 and 2007. However, instrumentation has been secured with support from PASSCAL such that a total of seven new arrays (see Figure 1 and Table 1) will be installed by the end of September 2010. Four of these new arrays have been installed to date. Data from all arrays are telemetered in near-real-time to the University of Utah and archived at the Incorporated Research Institutions for Seismology's Data Management Center (IRIS DMC) for easy access by all members of the research group. The data are also archived to DVD at the University of Utah.

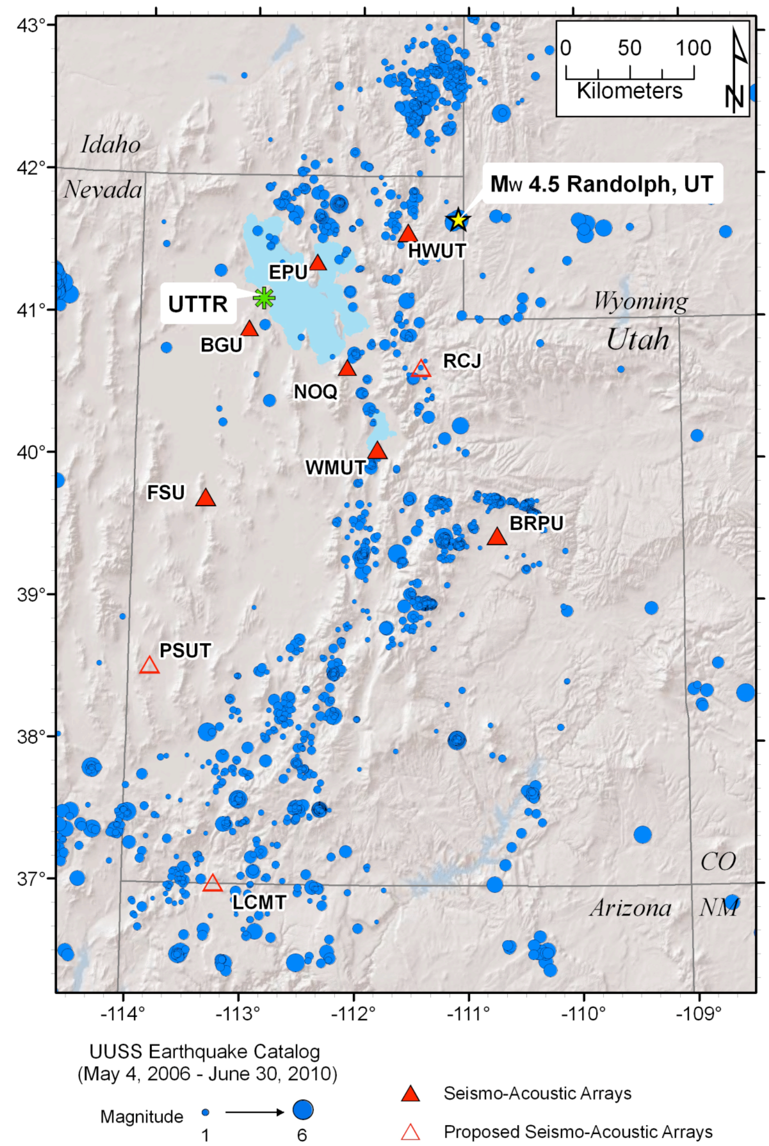

Figure 1. Study area with locations of infrasound arrays and earthquakes M > 1.5 located by the University of Utah seismograph stations between 5/4/2006 and 6/30/2010 (N = 4381). Earthquakes are scaled by magnitude. The seismicity immediately north and west of array BRPU is related to underground coal mining and will not be included in this study. The two events analyzed (Randolph earthquake and the Utah Test and Training Range detonation) are also shown.

Each station consists of four acoustic sensors, with ~100 m spacing, with one acoustic sensor being collocated with a seismic sensor. Figure 2 shows the location and sensor distribution for the array WMUT, which is representative of the general layout of each array in the network. See Table 1 for a complete list of the sensors and telemetry for each array.

The three arrays installed in 2006 and 2007 use Chaparral 2 and Chaparral 2.5c sensors modified by Southern Methodist Univeristy (SMU) to operate on 12 volts rather than 24 volts. This modification includes reducing the sensitivity of the unit from 400 mV/Pa to 200 mV/Pa. Nominal response and self-noise remain the same. In 2006, prior to installation, SMU matched the sensor phase response such that the phase mismatch among the Chaparral sensors in an array was less than 10° in the 0.1- to 5-Hz band. While we expect that the mismatch above 5 Hz is well within 10°, this was not confirmed with laboratory tests.

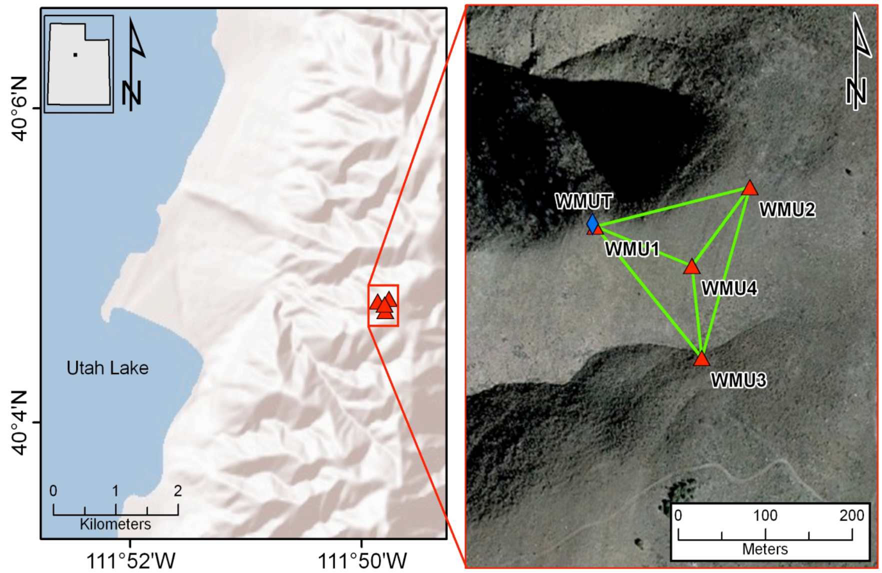

Figure 2. Left: Location of seismo-acoustic array WMUT acoustic sensors shown as red triangles. Right: Overhead view of WMUT acoustic array configuration with ~100 m spacing and northwest element (WMU1) collocated with an existing seismometer (blue diamond).

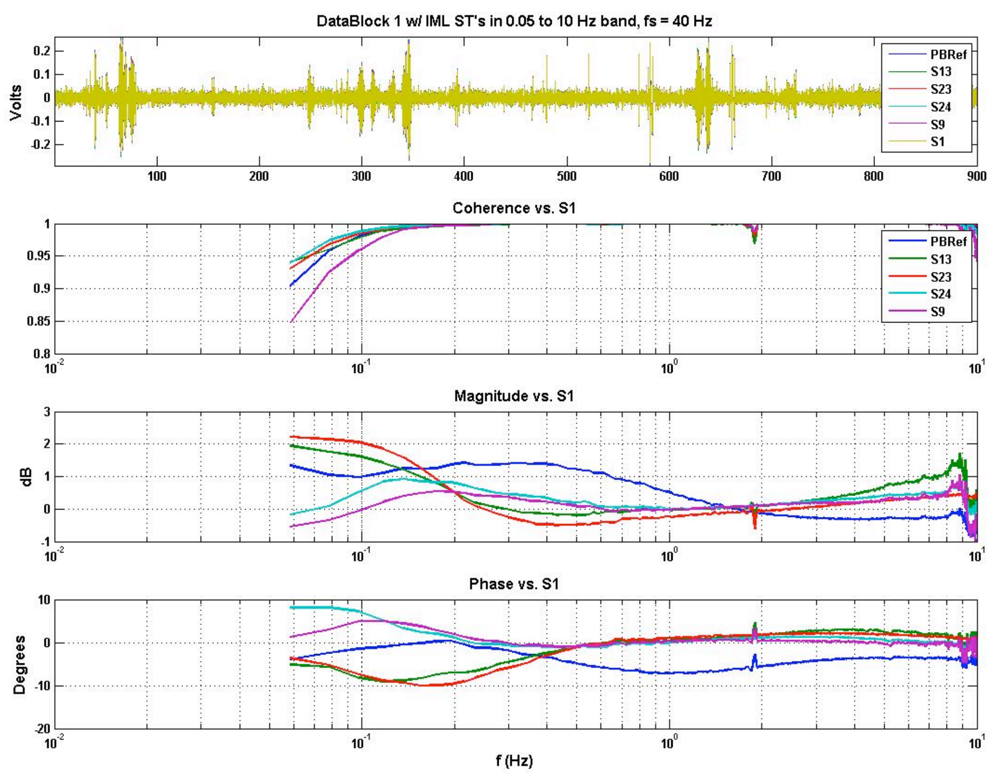

Figure 3. Relative responses of one group of Inter-Mountain Laboratories (IML) sensors from IML's in-house testing and adjustment. The dark blue is a laboratory reference IML used for tracking differences between groups of sensors. (Figure provided by IML.)

For arrays using Chaparral sensors, the sensors are connected to 10-port manifolds with Fiskars-brand 25-ft, 5/8-in. soaker hoses on each port. This forms the standard wind noise filter. Because the original Fiskars-brand hoses are no longer available, the hoses on the existing arrays have not been replaced since installation. In other locations, aging hoses sometimes result in additional wind noise due to cracks and holes in the hose. Thus, it is important to recognize the difference between a detection failure due to low or no signal as opposed to a wind noise–blinded conditions.

The arrays installed under this project use IML Seattle-T (IML-ST) sensors, an improved sensor relative to the earlier IML Seattle-S sensor used as part of an infrasound avalanche detector. Although the IML does not have the flat low-frequency response of the Chaparral, previous tests of the IML Seattle-S sensor by SMU and by Sandia have indicated that it is useful down to 0.10 Hz and up to at least 10 Hz. The IML-ST model has an improved response and is suitable for direct connections to digitizers. The IML models used for this project use 8-port manifolds with the same 25-ft Fiskars-brand hoses.

The IML-ST systems were ordered from IML with a requested phase match at 0.5 Hz. IML sorted the sensors into six groups of four sensors and then adjusted the phase response of the sensors to match within 5° at 0.5 Hz and 3-dB amplitude at 1 Hz (Figure 3). In review, most of the groups were matched better than these nominal values.

Table 1. Instrumentation

	Seismometer	**Microphones**	**Telemetry**	**Install Date**
NOQ	Broadband Nanometrics Trillium 120	Chaparral 2	RADIO	May 4, 2006
BGU	Broadband Nanometrics Trillium 120	Chaparral 2	RADIO	April 17, 2007
EPU	Short-period vertical Mark Products L-4C	Chaparral 2.5	RADIO	July 13, 2007
BRPU	Broadband Nanometrics Trillium 240	Inter-Mountain Labs Model ST	CELL MODEM	April 16, 2010
WMUT	Short-period Vertical Mark Products L-4C	Inter-Mountain Labs Model ST	CELL MODEM	May 8, 2010
HWUT	Broadband Streckheisen STS-2	Inter-Mountain Labs Model ST	RADIO	May 14, 2010
FSUT	Short-period Vertical Mark Products L-4C	Inter-Mountain Labs Model ST	RADIO TO A CELL MODEM	June 10, 2010
PSUT	Broadband Nanometrics Trillium 120	Inter-Mountain Labs Model ST **	RADIO OR CELL MODEM	Planned for July 2010
LCMT	Broadband Guralp CMG-3T	Inter-Mountain Labs Model ST**	RADIO OR CELL MODEM	Planned for July 2010
RCJ*	Short-period vertical Geotech S-13	Inter-Mountain Labs Model ST**	RADIO OR CELL MODEM	Planned for September 2010

** RCJ or nearby site* ***Planned sensors*

SMU duplicated IML's response results, and compared responses to an additional Chaparral 2.5 sensor that has been used as a reference in adjusting the Chaparrals at the three 2006 arrays and to a Setra Model 239 as a reference to absolute pressure. These results will be incorporated into the SEED dataset header for the delivered datasets.

Data Processing

Continuous data for all arrays are being processed using the Los Alamos National Laboratory InfraMonitor software package (Arrowsmith and Whitaker, 2008). The software uses multiple arrays to detect, associate, and locate infrasound-generating sources. A strength of InfraMonitor is its use of an adaptive noise approach to account for variations in ambient noise. The spatial and azimuthal distribution of the network of arrays with respect to the seismic zone increases the likelihood of acquiring multiple array detections and provides tighter constraints on the infrasound source location (increased number of crossing backazimuths), which is needed to obtain robust associations with seismic events.

For the purpose of example, we have processed two days of data and report on the analysis of two events. The first day, April 16, 2010, contains the recordings from a local M_W-4.5 earthquake located near Randolph, Utah. The second day, June 28, 2010, contains a rocket motor detonation at the Utah Test and Training Range (UTTR). This ground-truth event is used for calibration.

Randolph Earthquake

The Randolph earthquake (M_W 4.5) was the largest recorded earthquake located in the state of Utah since 1992. The earthquake was widely felt throughout northern Utah and parts of Wyoming and Idaho. It was a normal faulting event on a generally north-striking fault (Hermann, undated) and reportedly produced local liquefaction features. Peak horizontal and vertical accelerations (peak ground acceleration [PGA]) recorded at the closest station for this event (HWUT, Δ = 38km) were 0.7% g and 0.2% g, respectively. Using the Pankow and Pechmann (2004) ground-motion relation and the distribution of observed maximum horizontal PGA, the predicted horizontal ground motion at the source approaches 10% g (Figure 4). For an earthquake of this magnitude, the linear relations developed by Le Pichon et al. (2006) predict an infrasound signal with an amplitude of ~0.04 µbars and a duration of ~6 minutes for stratospheric returns.

No infrasound-generated waves were detected for this event at any of the three arrays operational in Utah (BGU, EPU, and NOQ), with distances varying from 115 km to 185 km to the earthquake epicenter. Ground-to-space (G2S) atmospheric profiles extracted for this date at the location of the epicenter (see Figure 1) are shown in Figure 5 for each of the three arrays. The three profiles have been computed by summing the wind in the direction of propagation with the sound speed due to temperature. In order to form a duct, the effective sound speed must exceed the sound speed at the surface (~350 m/s). For this date and location, this only occurs in the thermosphere (~110 km), which would produce returns at horizontal distances greater than those separating the epicenter and the operational arrays. Given the atmospheric conditions, even if the Randolph earthquake generated strong infrasound, the probability of detection by these three arrays would be very low. Had the array at BRPU (distance ~250 km) been installed one day earlier—since the effective sound speed along that path in the stratosphere is greater than for the other arrays (Figure 5)—the probability of detection would have been greater. However, no duct is predicted for that path either, based purely on the unperturbed G2S model. Since the earthquake was located at the edge of our network, the azimuths to each array are similar (south–southwest), and path effects, therefore, are similar. Thus, if path effects are unfavorable, in this case, they are unfavorable to all arrays. This clearly validates our strategy of deploying a dense network of arrays to ensure that the Intermountain Seismic Belt in Utah is well sampled at different directions and azimuths.

Utah Test and Training Range Blast

The UTTR blast was well recorded at five of seven arrays operational at the time of detonation (Figure 6) and was used as a calibration source for the new instrumentation. Array EPU was operating but not telemetering due to vandalism, and array NOQ did not detect the event. Figure 7 shows the data from WMUT processed with

InfraMonitor. At the expected time for epicentral infrasonic arrivals (green bars), there is a peak in both the correlation and F-statistic (Blandford, 1974) parameters corresponding to these arrivals. The backazimuth is also consistent with the known location of the UTTR blast zone. To take advantage of the network of infrasonic arrays, the backazimuth estimate and the infrasonic arrival times from WMUT are combined with the results determined from the four other arrays that detected the blast using the Bayesian Infrasound Source Location (BISL) algorithm developed by Modrak et al. (2010). The results are presented in Figure 8 and provide confirmation of the validity of the algorithm, the success of the array installations, and the accuracy of array metadata. The regions enclosed by the credibility contours are 135 km^2 (at 0.75), 391 km^2 (at 0.9) and 610 km^2 (at 0.95).

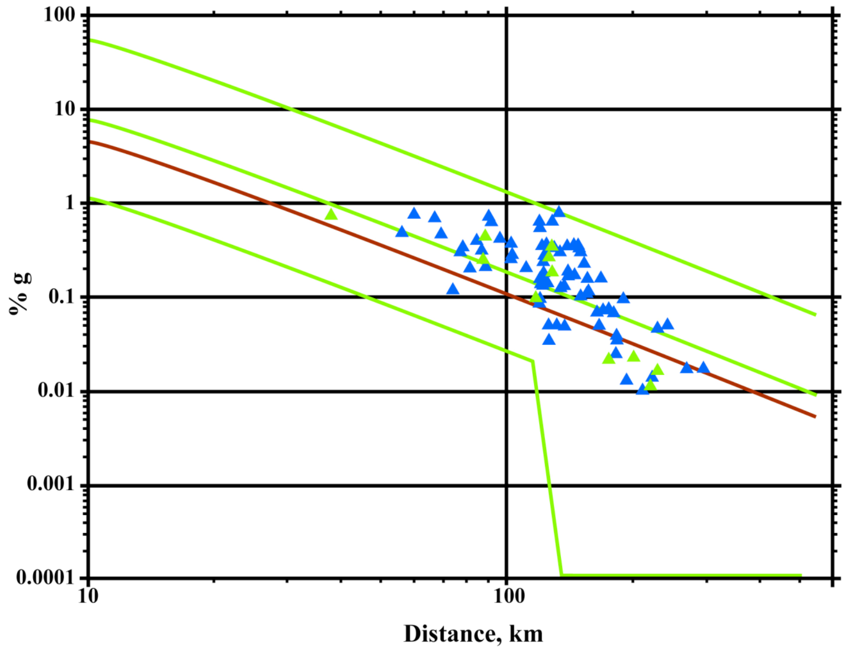

Figure 4. Distribution of maximum horizontal PGA recorded by the Utah Regional Seismic Network (blue triangles = UU stations; green triangles = US and NP stations) for the Randolph earthquake. The red line is the ground motion as a function of distance predicted by Pankow and Pechmann (2004). The green lines are the ground-motion prediction and standard deviation determined by adjusting for the calculated bias in the distribution of measured PGA. This is the method used in ShakeMap (Wald et al., 2005).

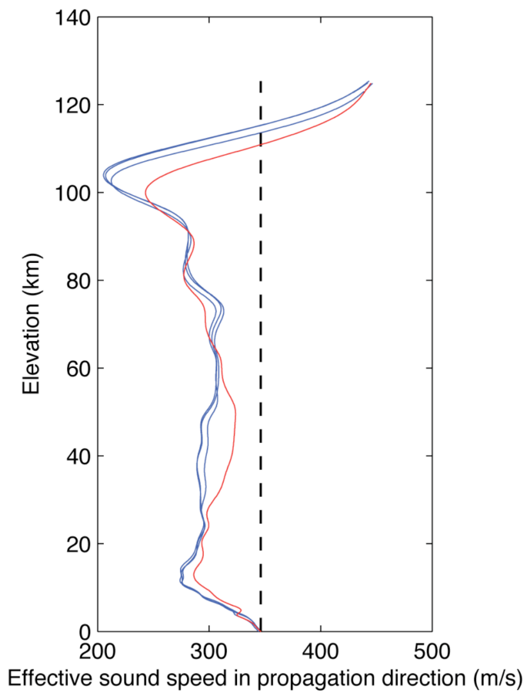

Figure 5. Ground-to-space profiles for April 16, 2010, 00:00 UTC, at the location of the Randolph earthquake epicenter. The three profiles for BGU, EPU, and NOQ (blue) and BRPU (red) have been computed by summing the wind in the direction of propagation with the sound speed due to temperature. The dashed bar represents the sound speed at the ground that must be exceeded to expect local-to-regional returns.

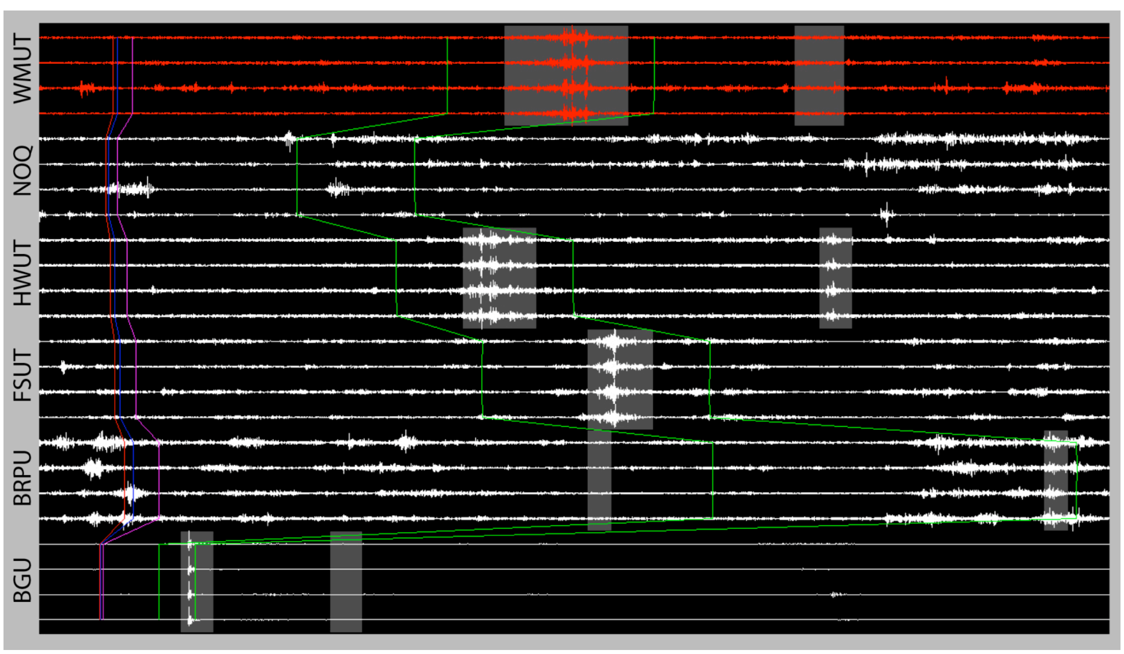

Figure 6. InfraMonitor output of acoustic data recorded from a UTTR blast on June 28, 2010. Expected times for seismic and infrasonic arrivals are denoted by purple and green colored lines, respectively.

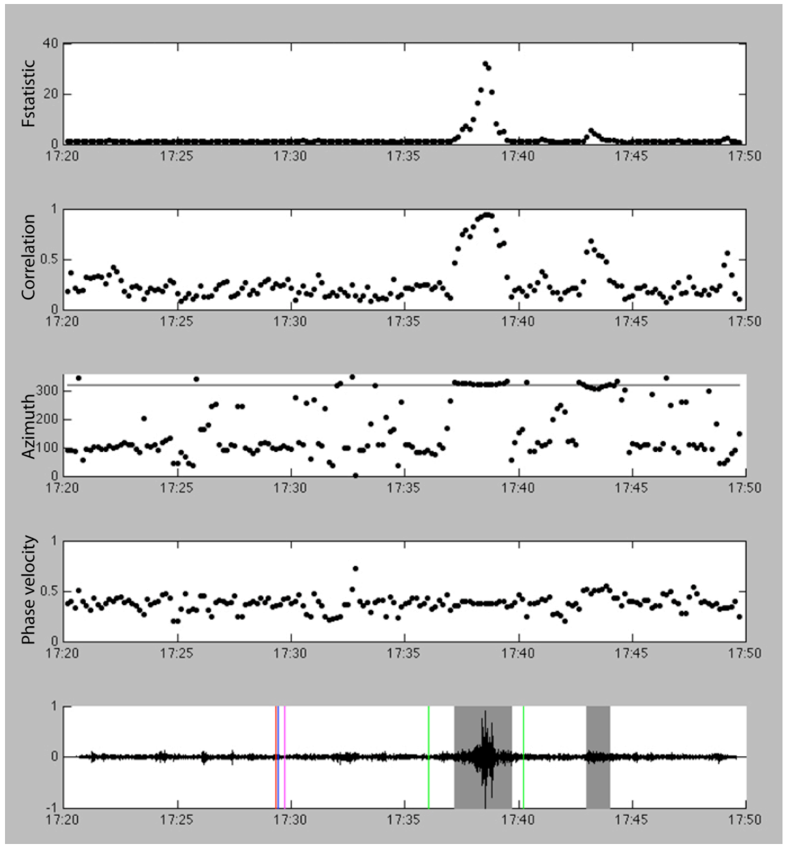

Figure 7. InfraMonitor plot showing the array processing of the June 28, 2010, UTTR blast, recorded at WMUT. The lower panel shows the normalized beam trace (filtered from 1–5 Hz), and the upper four panels show the InfraMonitor-derived array parameters. The purple bars show the expected seismic arrivals, while the green bars show the expected time of epicentral infrasonic arrivals.

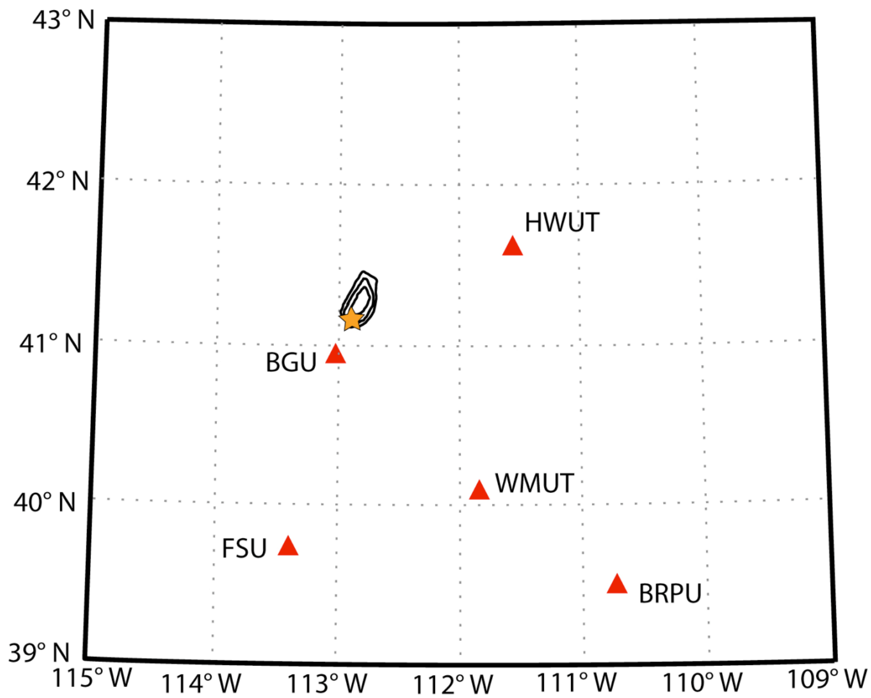

Figure 8. Location of the June 28, 2010, UTTR blast, determined using the BISL algorithm. Triangles show locations of arrays contributing to the location. The source location is shown as 75%, 90%, and 95% credibility contours from the algorithm. The star symbol represents the ground-truth detonation location.

CONCLUSIONS AND RECOMMENDATIONS

The major focus of the first year has been deployment of infrasound arrays, collocated with seismometers within the Utah Regional Seismic Network. When completed, the Utah infrasound network (seven new and three existing arrays) will consist of the most densely spaced local seismo-acoustic array network to date. The arrays are located within a seismic zone, making it possible for possible local infrasonic arrivals, previously overlooked, to be studied. Data from each of the arrays either are or will be telemetered in near-real-time to the University of Utah, where they will be processed and archived at the IRIS-DMC. While the density does not change the likelihood of an infrasound-generating earthquake occurring, the spatial coverage will provide a greater possibility of obtaining multiple observations from smaller earthquakes than in past studies. Continuous data from 2006 to the present are being processed with InfraMonitor in order to generate both lists of detections and catalogs of infrasound source locations using the smaller three-array infrasound network. We provide examples from both an explosion and an earthquake, utilizing data from the new arrays, which confirm that the array installations to date have been successful. Future work will concentrate on the continued processing of the continuous infrasound data and the correlation of identified signals with source characteristics and earthquake ground motions to further refine the source excitation model for infrasound from earthquakes.

ACKNOWLEDGEMENTS

We would like to thank the following for their assistance and continued support throughout this project: Mike Thorne, Dave Drobeck, Peter O'Neill, Wesley O'Keefe, Hans Andersen and William Pomerleau. Dataloggers and materials support are being provided by PASSCAL.

REFERENCES

Arrowsmith, S. J. and R. Whitaker (2008). InfraMonitor: A tool for regional infrasound monitoring, in *Proceedings of the 30th Monitoring Research Review: Ground-Based Nuclear Explosion Monitoring Technologies,* LA-UR-08-05261, pp. 837–843.

Arrowsmith, S. J., R. Whitaker, S. R. Taylor, R. Burlacu, B. Stump, M. Hedlin, G. Randall, C. Hayward, and D. ReVelle (2008). Regional monitoring of infrasound events using multiple arrays: Application to Utah and Washington State, *Geophys. J. Int.* 175: 291–300.

Blandford, R. R. (1974). An automatic event detector at the Tonto Forest Seismic Observatory, *Geophysics* 39: 633–643.

Che, I.-Y., M.-S. Jun, J.-S. Jeon, and K. Min (2002). Analysis of seismo-acoustic events in the Korean Peninsula. *Geophys. Res. Lett.* 29.

Garcés, M., R. Hansen, and K. Lindquist (1998). Traveltimes for infrasonic waves propagating in a stratified atmosphere, *Geophys. J. Int*. 135: 255–263.

Hermann, R. B. (undated, accessed July 2010). Focal mechanism determinations for U.S. http://www.eas.slu.edu/Earthquake_Center/recenteq.html

Kim, T. S., C. Hayward, and B. Stump (2004). Local infrasound signals from the Tokachi-Oki Earthquake, *Geophys. Res. Lett.* 31: L20605 10.1029/2004GL021178.

Le Pichon, A., P. Mialle, J. Guilbert, and J. Vergoz (2006). Multistation infrasonic observations of the Chilean earthquake of 2005 June 13, *Geophys. J. Int.* 167: 838–844.

McKenna, M. H., B. W. Stump, S. Hayek, J. R. McKenna, and T. R. Stanton (2007). Tele-infrasonic studies of hard-rock mining explosions, *J. Acoust. Soc. Am.* 122: 97–106.

Modrak, R. T., S. J. Arrowsmith, and D. N. Anderson (2010). A Bayesian framework for infrasound location, *Geophys. J. Int*. 181: 399–405.

Mutschlecner, J. P. and R. W. Whitaker (2005). Infrasound from earthquakes, *J. Geophys. Res.* 110: D01108, doi:10.1029/2004JD0050067.

Pankow, K. L. and J. C. Pechmann (2004). The SEA99 ground-motion predictive relations for extensional tectonic regimes: Revisions and a new peak ground velocity relation, *Bull. Seism. Soc. Am.* 94: 341–348.

Smith, R. B. and W. J. Arabasz (1991). Seismicity of the intermountain seismic belt, in *Neotectonics of North America*, D. B. Slemmons, E. R. Engdahl, M. L. Zoback, and D. D. Blackwell, Eds. Boulder, CO: Geol. Soc. Am.

Sorrells, G. G., E. Herrin, and J. L. Bonner (1997). Construction of regional ground-truth data base, *Seismo. Res. Lett.* 68: 743–752.

Stump, B., R. Burlacu, C. Hayward, K. Pankow, S. Nava, J. Bonner, S. Hock, D. Whiteman, A. Fisher, T. S. Kim, R. Kubacki, M. Leidig, J. Britton, D. Drobeck, P. O'Neill, K. Jensen, K. Whipp, G. Johnson, P. Roberson, R. Read, R. Brogan, and S. Masters (2007). Seismic and Infrasonic Energy Generation and Propagation at Local and Regional Distances: Phase I—Divine Strake Experiment, Air Force Research Laboratory report, AFRL-RV-HA-TR-2007-1188.

Stump, B., Hayward C., Arrowsmith S., Randall G., Pankow K., Burlacu R., and Taylor S. R (2009). Infrasound from earthquakes: Signal characterizations, in *Proceedings of the 2009 Monitoring Research Review*: *Ground-Based Nuclear Explosion Monitoring Technologies,* LA-UR-09-05276, Vol. 2, pp. 742–749.

Wald, D. J., B. C. Worden, V. Quitoriano, and K. L. Pankow (2005). *ShakeMap Manual: Technical Manual, User's Guide, and Software Guide*. U. S. Geological survey.